Electronic Supplementary Material (ESI) for Polymer Chemistry.
This journal is © The Royal Society of Chemistry 2014

Supporting Information

Pulsed-laser and Quantum Mechanics Study of *n*-Butyl Cyanoacrylate and Methyl Methacrylate Free-Radical Copolymerization

Thomas R. Rooney, Evangelos Mavroudakis, Igor Lacík, Robin A. Hutchinson,* and Davide Moscatelli*

Copolymer Composition Characterization.

When methanol (MeOH) containing 5 v% methacrylic acid (MAA) is used to treat the PLP reaction mixture the FRP-generated copolymer can be successfully isolated devoid of anionic PBCA. A typical ^{1}H-NMR spectrum of the isolated copolymer is shown in Figure S1. The total moles of copolymer can be measured using two separate methods, represented by Equations S1 & S2, which are derived from three independent signals such that three independent estimates of copolymer composition can be made per sample via Equations S3, S4, and S5. The peak integration used to formulate Equation S1 comprises an overlap of signals with identical multiplicities originating from both methyl methacrylate (MMA) and *n*-butyl cyanoacrylate (BCA) pendant chains. By comparing Equations S1 & S2 one can see that the presence of any anionic PBCA will lead to a distinct disagreement between the two measures and consequently an unreliable estimate of copolymer composition. The three calculations are summarized in Table S1 for a range of initial BCA content samples. The estimate from Equation S3 was used for the Mayo-Lewis plot in the **Results and Discussion** section because it uses one independent peak from each pendant chain.

$$Pol_{Total,1} = \frac{Peak\ (d+q)}{3} \quad \text{(S1)}$$

$$Pol_{Total,2} = \frac{Peak\ a}{2} + \frac{Peak\ e}{3} \quad \text{(S2)}$$

$$F_{BCA}(S3) = \frac{\frac{Peak\ a}{2}}{Pol_{Total,2}} \quad \text{(S3)}$$

$$F_{BCA}(S4) = \frac{\frac{Peak\ a}{2}}{Pol_{Total,1}} \quad \text{(S4)}$$

$$F_{BCA}(S5) = 1 - \frac{\frac{Peak\ e}{3}}{Pol_{Total,1}} \quad \text{(S5)}$$

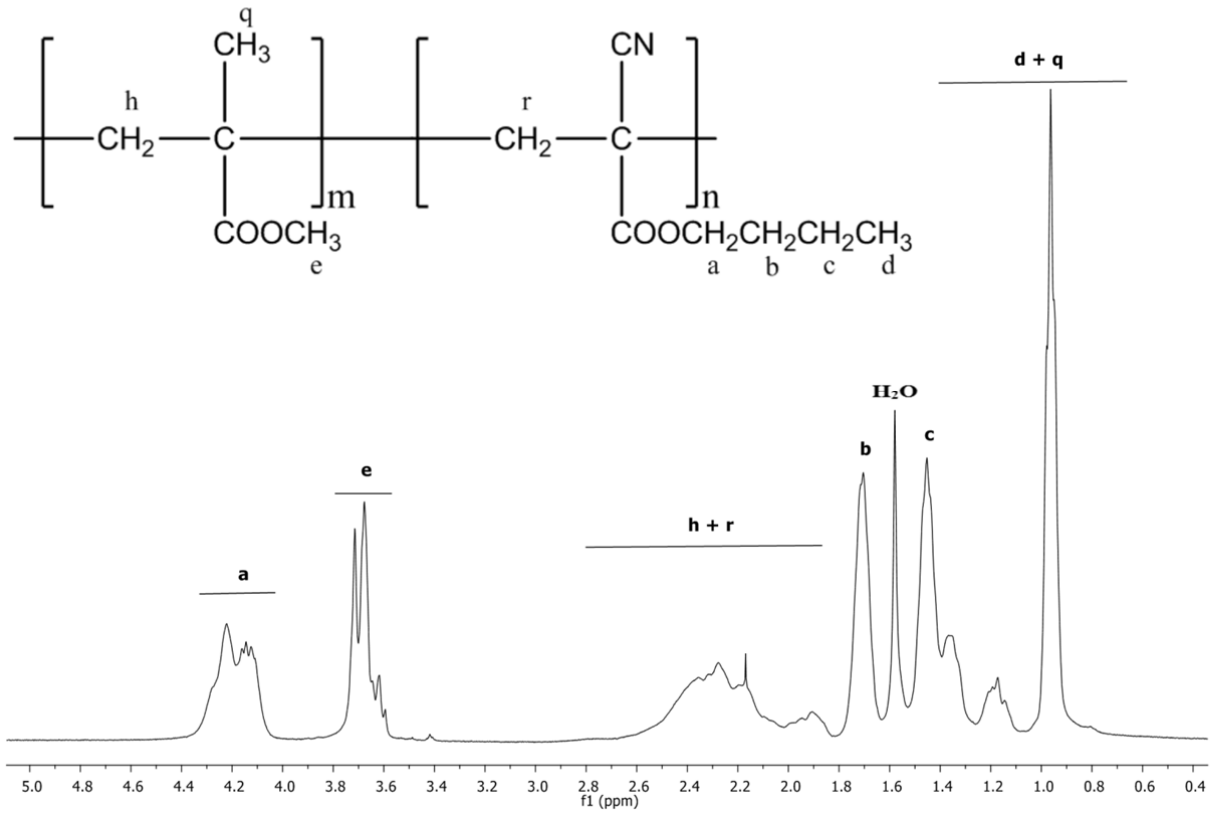

Figure S1. ^{1}H-NMR spectrum in $CDCl_3$ for a low-conversion (1.3 %) copolymer in which inadvertent anionic polymerization of BCA monomer was successfully suppressed during FRP and the copolymer isolation procedure. The copolymer was produced from f_{BCA}=0.72 in bulk at 50 °C at 50 Hz with 1 v% DCAA and 5 mmol·L^{-1} DMPA. Sample precipitation performed in MeOH containing 5 v% MAA at room temperature.

Table S1. Summary of three independent copolymer composition estimations made per low-conversion BCA/MMA copolymer generated at various temperatures by PLP.

Temperature	f_{BCA}		**Consistency Checks**	
(°C)		F_{BCA} **(S3)**	F_{BCA} **(S4)**	F_{BCA} **(S5)**
50	0.03	**0.30**	0.29	0.30
	0.07	**0.34**	0.34	0.34
	0.14	**0.43**	0.44	0.43
	0.14	**0.41**	0.41	0.41
	0.14	**0.45**	0.40	0.51
	0.22	**0.47**	0.49	0.44
	0.22	**0.47**	0.47	0.47

	0.22	**0.46**	0.43	0.50
	0.30	**0.50**	0.50	0.51
	0.40	**0.51**	0.49	0.52
	0.40	**0.50**	0.48	0.52
	0.40	**0.50**	0.46	0.53
	0.40	**0.52**	0.54	0.49
	0.50	**0.55**	0.55	0.56
	0.50	**0.56**	0.56	0.56
	0.50	**0.54**	0.53	0.55
	0.60	**0.60**	0.59	0.60
	0.60	**0.63**	0.65	0.62
	0.72	**0.61**	0.57	0.63
	0.72	**0.63**	0.64	0.62
	0.72	**0.63**	0.61	0.64
	0.85	**0.68**	0.66	0.68
	0.85	**0.68**	0.66	0.70
	0.85	**0.68**	0.67	0.68
30	0.03	**0.31**	0.29	0.33
	0.07	**0.38**	0.35	0.42
	0.14	**0.45**	0.42	0.48
	0.22	**0.48**	0.46	0.50
	0.50	**0.54**	0.51	0.57
70	0.03	**0.28**	0.27	0.30
	0.14	**0.43**	0.45	0.41
	0.40	**0.53**	0.49	0.56
	0.85	**0.69**	0.66	0.70

Composition-averaged Copolymer Propagation Rate Coefficient Estimation

Dichloroacetic acid (DCAA) is added in the amount of 1 v% to each BCA/MMA reaction mixture to suppress the anionic polymerization of BCA during the PLP experiment. In order to confirm that the presence of DCAA does not have an influence on the FRP kinetics of the BCA/MMA system, a set of PLP copolymerization experiments (f_{BCA}=0.03) were performed in bulk at 50 °C and 50 Hz in which the amount of DCAA was systematically varied from 0.1 to 3.0 v%, and MMA bulk homopolymerizations at 50 °C and 50 Hz were conducted with and 0 and 1 v% DCAA. The MWDs from these PLP-SEC experiments are presented in Figure S2 and do not demonstrate any significant dependence on DCAA content. This conclusion is supported by the results in Table S2 which show that there is no significant variation in $k_{p,cop}$ or $k_{p,MMA}$ with DCAA content.

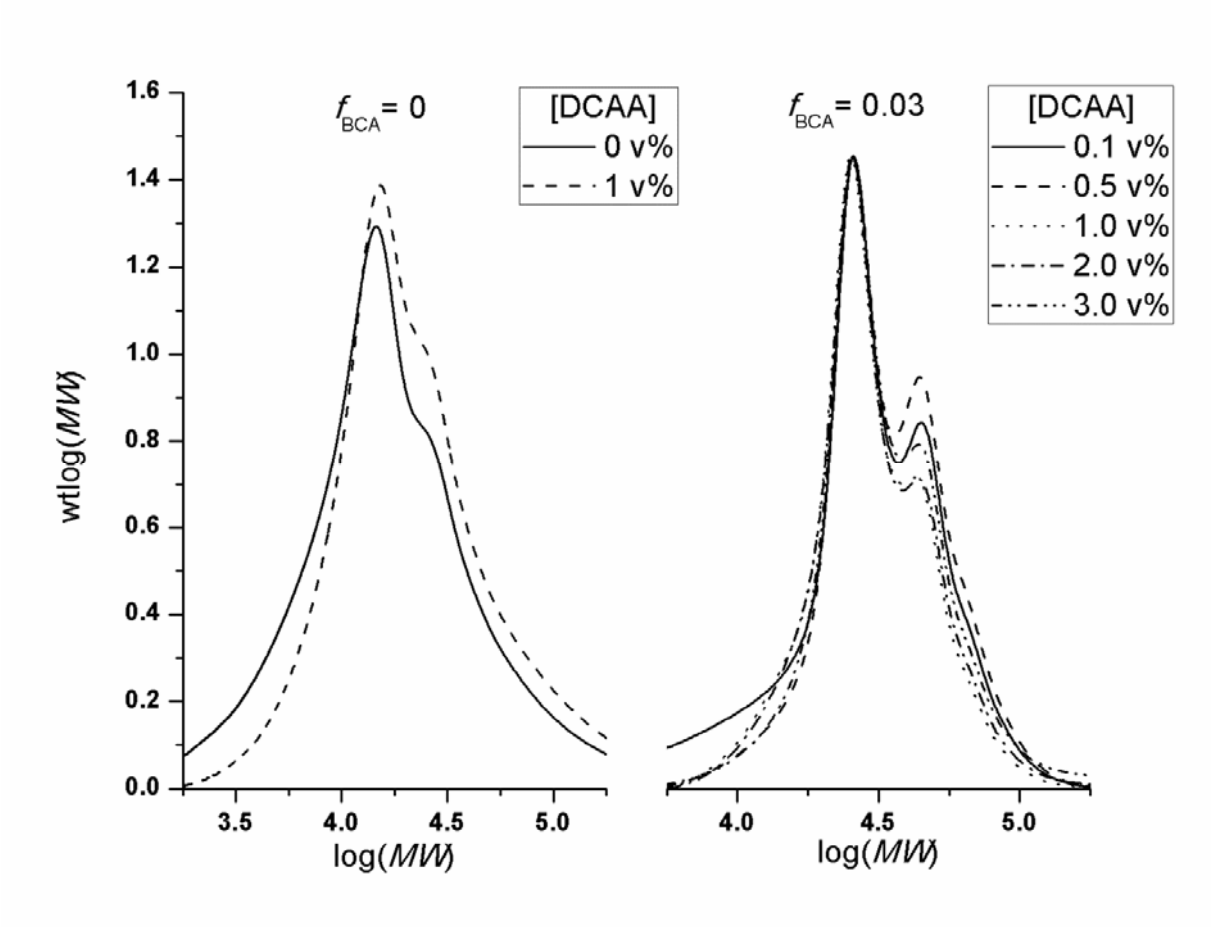

Figure S2. Effect of [DCAA] on MWDs generated from PLP experiments performed in bulk at 50 °C and 50 Hz with 5 mmol·L^{-1} DMPA.

Table S2. Effect of the presence of DCAA during PLP experiments performed at 50 Hz and 50 °C. Results are presented from RI detector relative to k_p estimated for MMA without any DCAA under identical operating conditions.

DCAA content (%v)	$k_{p,cop}([DCAA)/k_{p,MMA}$	
	$f_{BCA} = 0.03$	$f_{BCA} = 0$
0.0	-	1.00
0.1	1.98	-
0.5	1.95	-
1.0	1.95	1.02
2.0	1.99	-
3.0	2.01	-

The estimates which were deemed reliable from the BCA/MMA PLP-SEC experiments, performed at 50 °C with 1 v% DCAA and 5 mmol·L^{-1} DMPA, to construct the $k_{p,cop}$ plot in the **Results and Discussion** section and subsequently used to extrapolate an estimated value for $k_{p,BCA}$ are presented in Table S4. Although FRP polymer was recovered from f_{BCA}=0.93 PLP experiments and ^{1}H-NMR analysis confirmed the incorporation of some MMA units, the amount and sensitivity of contaminant PBCA production is overwhelming and prevents accurate $k_{p,cop}$ estimation even from an array of different operating conditions. Figure S3 illustrates the difficulties in obtaining PLP structure from high f_{BCA} samples where the sample pulsed at 20 Hz was divided into two. One half was treated with a volume of precipitation solution (denoted by *) twice that of the other. When the amount of MeOH solution is doubled at -10 °C the high MW contaminant PBCA peak becomes more prominent and the low MW PLP structure is lost (remains in solution). The inflection point locations are provided in Table S3 and indicate that the $k_{p,cop}$ for f_{BCA}=0.93 is between 349 and 503 L·mol^{-1}·s^{-1}. Although this cannot be confirmed it is still consistent with the trend shown for the $k_{p,cop}$ plot in the **Results and Discussion** section.

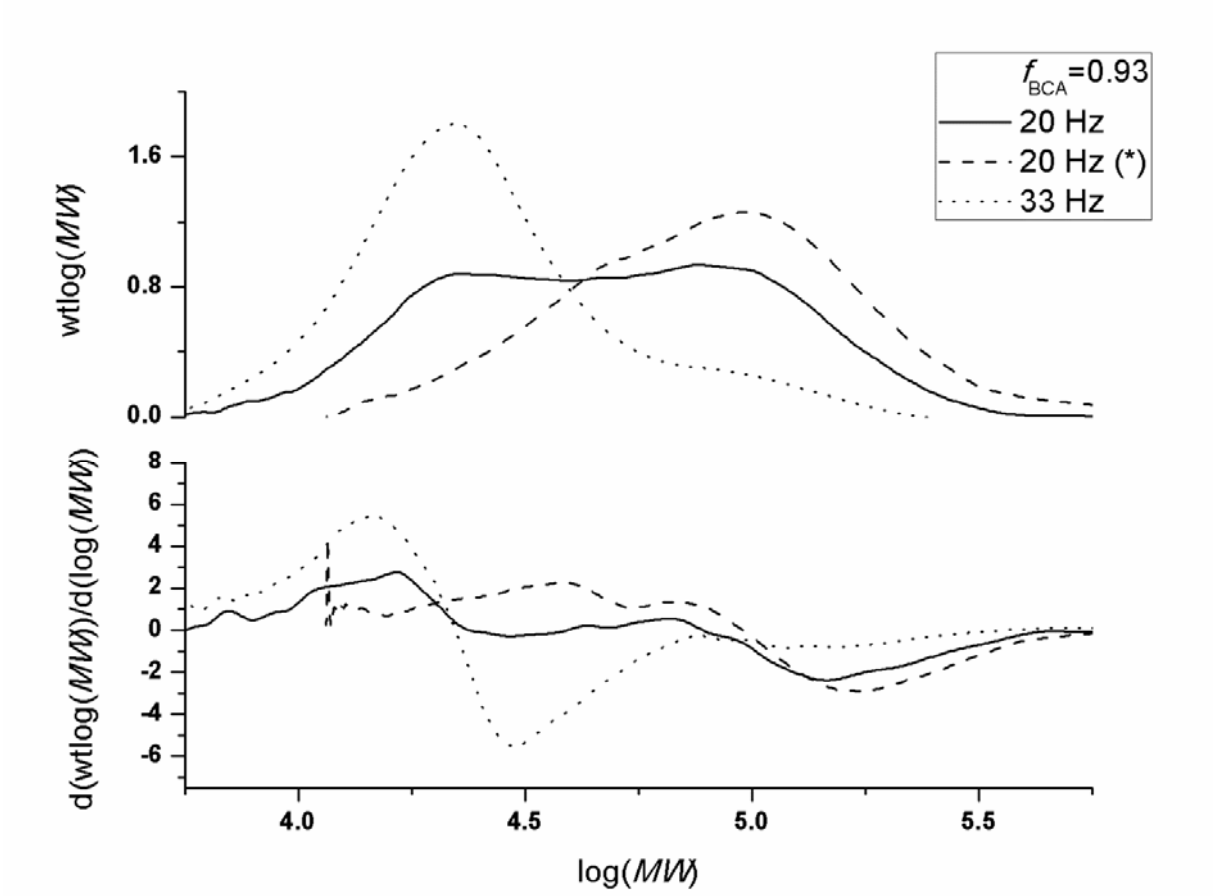

Figure S3. MWDs and 1st derivative plots for bulk BCA/MMA with 1 v% DCAA and 5 mmol·L^{-1} DMPA pulsed from f_{BCA}=0.93 at 50 °C. All samples were precipitated in MeOH containing 5 v% MAA at -10 °C. * indicates that twice the volume of precipitation solution was used to treat the sample.

Table S3. Inflection points corresponding to 1st Derivative plots in Figure S2 for f_{BCA}=0.93 pulsed at 50 °C with 1 v% DCAA and 5 mmol·L^{-1}. Samples were precipitated in MeOH containing 5 v% MAA at -10 °C. * indicates that twice the volume of precipitation solution was used to treat the sample.

	M_1 (g·mol^{-1})	M_2 (g·mol^{-1})	M_3 (g·mol^{-1})	M_2/M_1	M_3/M_2	$k_{p,cop}$ from M_1 (L·mol^{-1}·s^{-1})
20 Hz	16654	43733	66100	2.63	1.51	349
20 Hz*	38473	68470	-	1.78	-	806
33 Hz	14537	76213	-	5.24	-	503

A direct estimate of $k_{p,BCA}$ was not possible because the homopolymer undergoes depolymerization in THF while awaiting SEC analysis (even when the PLP reaction mixture is spiked with 2500 ppm MMA). As shown in Figure S4, MWDs without PLP features are obtained even when the PLP experiment is performed at 75 °C and 10 Hz (although in this case a degraded PLP distribution is apparent). At 50 °C there is only a high MW population and oligomers which is consistent with depolymerization-repolymerization behaviour.

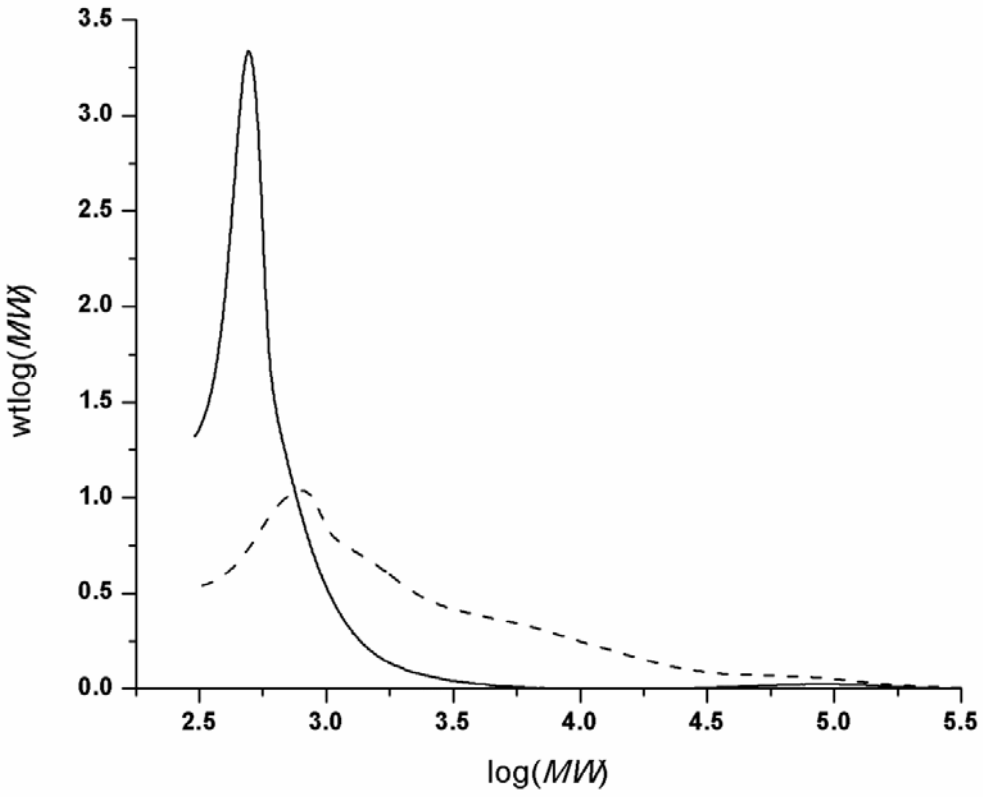

Figure S4. MWDs for BCA homopolymerization at 50 °C (solid line) and 75 °C (dashed line) 1 v% DCAA and 5 mmol·L^{-1} DMPA at 33 and 10 Hz, respectively.

Table S4. BCA/MMA PLP experimental conditions and results selected for $k_{p,cop}$ estimates with [DMPA] = 5 mmol·L^{-1} at 4-6 mJ/pulse. All experiments performed at Queen's University except the values in italics which were performed at the Polymer Institute SAS.

T (℃)	Pulse Repetition Rate (Hz)	f_{BCA}	F_{BCA}	Conversion %	SEC Results						
					RI			LS			$k_{p,cop,LS}/k_{p,cop,RI}$
					M_1 (g·mol^{-1})	M_2/M_1	$k_{p,cop}$ from M_1 (L·mol^{-1}·s^{-1})	M_1 (g·mol^{-1})	M_2/M_1	$k_{p,cop}$ from M_1 (L·mol^{-1}·s^{-1})	
30	33	0	0	0.3	9772	2.10	346	9484	2.18	336	0.97
30	20	0	0	0.3	15959	2.07	343	-	-	-	-
30	33	0	0	0.4	11099	2.06	393	-	-	-	-
30	20	0.03	-	0.2	32592	2.12	705	-	-	-	-
30	33	0.03	0.31	0.3	23384	1.94	827	-	-	-	-
30	20	0.07	-	0.3	40268	1.81	868	-	-	-	-
30	33	0.07	-	0.3	23702	2.23	843	-	-	-	-
30	33	0.07	0.38	0.2	27458	1.96	972	-	-	-	-
30	33	0.14	-	0.5	26031	2.05	921	-	-	-	-
30	33	0.14	0.45	0.4	29481	1.97	1043	-	-	-	-
30	33	0.22	0.48	0.5	30968	1.92	1096	-	-	-	-
30	33	0.50	0.54	0.5	25252	1.79	894	-	-	-	-
50	50	0	0	0.4	12769	1.89	703	14223	2.32	783	1.11
50	33	0	0	1.2	19059	1.88	692	18239	2.34	663	0.96
50	50	0.03	0.30	0.4	24748	2.00	1372	-	-	-	-
50	33	0.03	0.30	0.9	37137	2.01	1359	29785	2.98	1090	0.80
50	33	0.07	0.34	4.7	42936	2.00	1566	47863	2.08	1746	1.11
50	33	0.14	0.43	0.3	45738	1.98	1658	-	-	-	-
50	50	0.14	0.41	0.6	32859	2.01	1805	-	-	-	-
50	33	0.14	0.45	1.0	46151	2.03	1673	-	-	-	-
50	33	0.22	0.47	1.1	48149	1.88	1735	-	-	-	-
50	33	0.22	-	0.6	45686	1.99	1646	53088	1.98	1912	1.16
50	25	0.22	-	0.2	58552	2.03	1598	71779	1.88	1959	1.23

50	50	0.22	-	1.0	32136	1.97	1754	30761	2.19	1679	0.96
50	50	0.30	0.50	2.0	31894	1.81	1730	30549	1.98	1657	0.96
50	33	0.40	-	3.1	44872	1.97	1596	47424	1.95	1687	1.06
50	50	0.40	0.52	2.9	29509	1.93	1591	31989	2.16	1724	1.08
50	25	0.40	-	2.8	55121	2.05	1486	67143	1.90	1810	1.22
50	33	0.50	0.55	1.8	40694	1.92	1439	41591	2.00	1470	1.02
50	50	0.50	0.56	1.5	27127	2.00	1453	31769	2.08	1702	1.17
50	25	0.50	-	1.5	49006	2.16	1313	54325	2.01	1455	1.11
50	33	0.60	0.63	1.4	36589	1.80	1285	37931	1.86	1333	1.04
50	50	0.60	0.60	0.2	25645	2.10	1365	-	-	-	-
50	50	0.72	-	0.4	17818	2.23	942	23768	2.50	830	0.88
50	50	0.72	-	0.7	22082	1.84	1168	-	-	-	-
50	20	0.85	0.68	0.3	27508	2.06	578	-	-	-	-
50	100	0	-	1.6	6502	2.01	716	-	-	-	-
50	*50*	*0*	-	*1.4*	*12664*	*2.01*	*697*	-	-	-	-
50	*33*	*0*	-	*3.5*	*19872*	*1.83*	*722*	-	-	-	-
50	*20*	*0*	-	*3.4*	*30825*	*1.81*	*679*	-	-	-	-
50	*10*	*0*	-	*3.9*	*55012*	*1.86*	*606*	-	-	-	-
50	*33*	*0.03*	-	*0.7*	*38128*	*1.79*	*1395*	-	-	-	-
50	*50*	*0.03*	-	*0.3*	*26664*	*1.80*	*1508*	-	-	-	-
50	*50*	*0.03*	-	*0.2*	*26788*	*1.79*	*1500*	-	-	-	-
50	*50*	*0.03*	-	*1.8*	*26912*	*1.78*	*1478*	-	-	-	-
50	*50*	*0.03*	-	*0.8*	*26974*	*1.78*	*1488*	-	-	-	-
50	*50*	*0.5*	-	*0.8*	*29214*	*1.85*	*1565*	-	-	-	-
50	*33*	*0.5*	-	*2.3*	*42107*	*2.03*	*1489*	-	-	-	-
50	*50*	*0.6*	-	*0.6*	*26929*	*1.82*	*1433*	-	-	-	-
50	*33*	*0.6*	-	*2.3*	*37583*	*1.99*	*1320*	-	-	-	-
50	*33*	*0.72*		*1.6*	*33397*	*1.93*	*1166*	-	-	-	-
70	33	0.00	0	0.6	28599	1.98	1009	-	-	-	-
70	33	0.03	0.28	1.2	53429	2.15	1884	-	-	-	-

70	33	0.07	-	1	62421	2.19	2201	-	-	-	-
70	33	0.14	-	2.7	68153	2.23	2403	-	-	-	-
70	33	0.22	-	1.2	68065	2.24	2400	-	-	-	-

Conformational search

For the detection of the optimized geometries for reactants and products a large number of potential energy surfaces (PES) for the rotation of various dihedral was used. In particular, a linear search of all the possible dihedral rotations was performed at the B3LYP6-31G(d,p) level of theory using a rotation step of 10° to perform the dihedral rotation simulations. It is worth mentioning that the structural optimization of the *n*-butyl group of BCA was conducted only for the monomer, while the optimum geometry was used for the rest of the studied molecules.

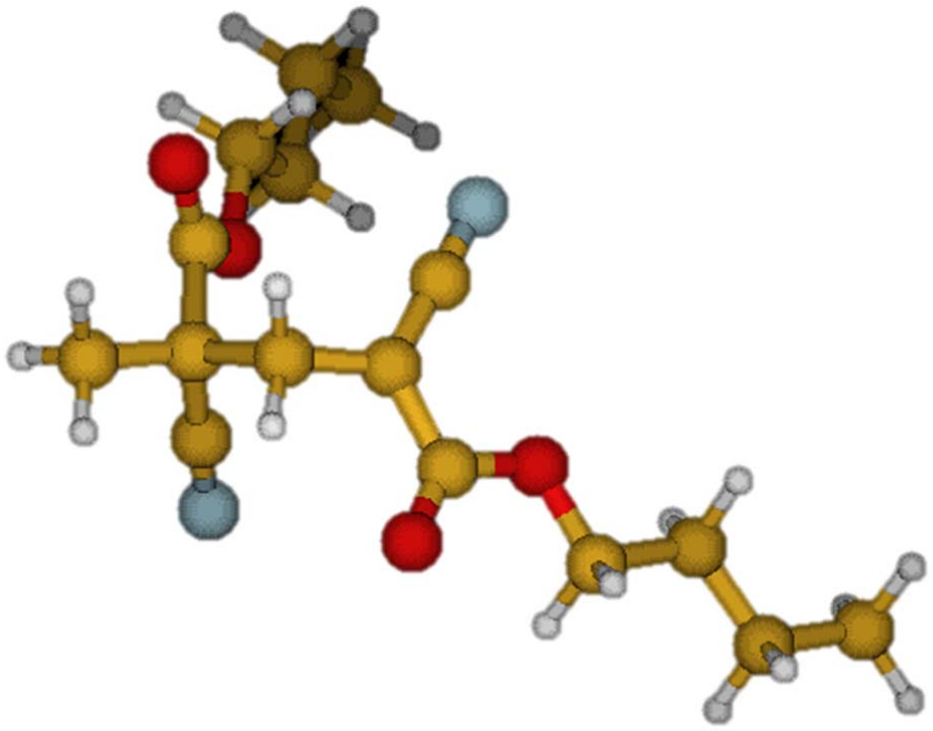

Figure S5: Minimum energy BCA dimer radical structure according to QM calculations

Atom coordinate details for the optimized transition state structures corresponding to the investigated propagation reactions.

BCA* + BCA →BCA_BCA*

C	-2.614955	-3.495579	-0.689205
C	-1.988336	-2.124436	-0.664652
C	-1.001884	-1.834849	-1.647665
N	-0.175436	-1.628349	-2.444734
C	-0.776809	-2.281440	1.225555
C	0.172226	-1.277805	1.268658
C	-0.118432	-0.002820	1.824697
N	-0.378398	1.032103	2.295774
C	-2.858359	-1.002977	-0.186220
O	-2.365066	0.196263	-0.514589
C	-3.102233	1.353129	-0.027841
C	-2.339850	2.595978	-0.450752
C	1.507430	-1.540930	0.648190
O	2.279975	-0.448366	0.639110
C	3.582373	-0.597702	0.015373
C	4.274765	0.753396	0.061604
O	-3.870197	-1.194276	0.462201
O	1.826022	-2.630598	0.215020
H	-3.280346	-3.580896	-1.558039
H	-1.859072	-4.279497	-0.770576
H	-3.223093	-3.643086	0.204641
H	-1.684666	-2.206495	1.812295
H	-0.426687	-3.266125	0.938015
H	3.433760	-0.952183	-1.009368
H	4.141371	-1.367411	0.557785
C	5.669209	0.705437	-0.576933
H	3.650386	1.491322	-0.456535
H	4.351007	1.082438	1.105280
H	-3.184761	1.275197	1.059866
H	-4.111583	1.318846	-0.450543
C	-3.054495	3.880933	-0.011040
H	-1.336997	2.558403	-0.010942
H	-2.216242	2.588820	-1.540822
C	-2.293583	5.146494	-0.416946
H	-4.064217	3.906207	-0.442741
H	-3.186206	3.868305	1.078726
H	-2.822060	6.048377	-0.092682
H	-1.294195	5.165698	0.030849
H	-2.171368	5.203990	-1.504294
C	6.381972	2.060534	-0.545579
H	6.283116	-0.043024	-0.058211
H	5.582550	0.361463	-1.616128
H	7.372173	1.998534	-1.007433
H	5.808814	2.821595	-1.086316
H	6.515038	2.414874	0.482513

BCA* + MMA →BCA_MMA*

C	4.179300	-0.435536	-0.250311
C	3.199718	0.724266	-0.313767
O	1.978068	0.303823	0.341345
C	0.984050	1.214338	0.377890
O	1.048380	2.321513	-0.120156
C	-0.237943	0.690849	1.054322
C	-1.315487	1.703933	1.353150
C	-0.974263	-0.421573	-0.716025
C	-2.224530	-0.944849	-0.445928
C	-2.431569	-2.275842	0.213011
C	-0.068190	-0.376618	1.983788
N	0.013851	-1.262357	2.738999
C	-3.394897	-0.101812	-0.796029
O	-4.565412	-0.731663	-0.540318
C	-5.747718	0.016718	-0.865712
O	-3.333265	1.022937	-1.264548
H	-0.913776	0.465557	-1.337577
H	-0.107932	-1.073167	-0.689101
H	3.583248	1.613788	0.196792
H	2.966044	1.011520	-1.344501
C	5.519268	-0.099133	-0.917741
H	4.340712	-0.708305	0.799654
H	3.728997	-1.310634	-0.735431
H	-2.963029	-2.167982	1.165652
H	-3.052437	-2.927853	-0.411953
H	-1.478882	-2.770511	0.409340
H	-5.765844	0.263711	-1.929997
H	-6.585386	-0.630286	-0.606998
H	-5.785942	0.944627	-0.289831
H	-0.973820	2.392935	2.135408
H	-1.541598	2.289018	0.461210
H	-2.224778	1.213790	1.705279
C	6.517165	-1.259409	-0.860027
H	5.345777	0.182782	-1.964861
H	5.956909	0.783884	-0.433251
H	7.464657	-0.992128	-1.338001
H	6.734035	-1.543513	0.175552
H	6.124482	-2.145597	-1.370687

MMA* + BCA →MMA_BCA*

C	4.157303	0.341533	0.079921
C	3.100257	-0.744466	-0.028410
O	1.881630	-0.124674	-0.506657
C	0.818089	-0.933518	-0.639589
O	0.821231	-2.124220	-0.384819
C	-0.378092	-0.203225	-1.146060
C	-0.316509	1.205876	-1.348187
N	-0.297968	2.358362	-1.522221
C	-1.538079	-0.906148	-1.370495
C	-2.844865	-0.986803	0.554112
C	-3.807780	-2.051281	0.117287
C	-3.321496	0.408138	0.393908
O	-2.579573	1.293763	1.094538
C	-2.926590	2.679886	0.911842
C	-1.858204	-1.326606	1.630423
O	-4.259574	0.729363	-0.319374
H	-2.370130	-0.448213	-1.890678
H	-1.478585	-1.987415	-1.337237
H	3.390730	-1.533842	-0.729766
H	2.896527	-1.219503	0.936942
C	5.500271	-0.206772	0.580420
H	4.286948	0.813005	-0.901843
H	3.795655	1.124333	0.757760
H	-1.147598	-0.518035	1.801049
H	-2.392200	-1.502262	2.576704
H	-1.309731	-2.241102	1.388366
H	-3.996480	2.829644	1.068591
H	-2.343987	3.225218	1.653585
H	-2.652320	3.005125	-0.094045
H	-4.373613	-1.743305	-0.763453
H	-3.297291	-2.999505	-0.075116
H	-4.537610	-2.237255	0.919782
C	6.573654	0.878831	0.701847
H	5.356772	-0.690409	1.555978
H	5.850625	-0.993577	-0.100900
H	7.520340	0.462788	1.060116
H	6.763936	1.357063	-0.265175
H	6.266330	1.662181	1.403271

MMA* + MMA →MMA_MMA*

C	0.997874	-0.221973	-0.950272
C	0.088614	0.736752	-1.333257
C	-1.450037	1.142788	0.273858
H	0.388389	1.776603	-1.276572
H	-0.705322	0.481456	-2.026725
C	-2.069213	2.380300	-0.316682
H	-2.865126	2.751827	0.345807
H	-1.333719	3.183803	-0.417497
H	-2.527670	2.175112	-1.285583
C	-0.632113	1.309623	1.523442
H	0.145089	2.065446	1.382876
H	-1.275895	1.641625	2.351853
H	-0.159972	0.375792	1.828789
C	0.796047	-1.691114	-1.193015
H	-0.117290	-1.866763	-1.766768
H	1.641095	-2.119399	-1.743053
H	0.726106	-2.245522	-0.250409
C	2.204386	0.243915	-0.231601
O	2.449133	1.402170	0.068321
O	3.046194	-0.780391	0.062935
C	4.248883	-0.403321	0.747605
H	4.804962	-1.328537	0.898917
H	4.831132	0.300519	0.147452
H	4.016825	0.065972	1.707128
C	-2.225771	-0.096681	0.066375
O	-3.087670	-0.243227	-0.787489
O	-1.859976	-1.098784	0.911465
C	-2.576174	-2.329348	0.738308
H	-2.406819	-2.741341	-0.259989
H	-2.188655	-3.005799	1.500319
H	-3.649544	-2.174582	0.873034